Atomic scale shot-noise using cryogenic MHz circuitry

F. Massee, Q. Dong, A. Cavanna, Y. Jin, and M. Aprili

Atomic scale shot-noise using cryogenic MHz circuitry

F. Massee,[1] Q. Dong,[2] A. Cavanna,[2] Y. Jin,[2] and M. Aprili[1]

[1]*Laboratoire de Physique des Solides (CNRS UMR 8502), Bâtiment 510, Université Paris-Sud/Université Paris-Saclay, 91405 Orsay, France*
[2]*Centre de Nanosciences et de Nanotechnologies, CNRS, Université Paris-Sud, Université Paris-Saclay, C2N—Marcoussis, 91460 Marcoussis, France*

By implementing dedicated cryogenic circuitry operating in the MHz regime, we have developed a scanning tunneling microscope (STM) capable of conventional, low frequency (<10 kHz), microscopy as well spectroscopy and shot-noise detection at 1 MHz. After calibrating our AC circuit on a gold surface, we illustrate our capability to detect shot-noise at the atomic scale and at low currents (<1 nA) by simultaneously measuring the atomically resolved differential conductance and shot-noise on the high temperature superconductor $Bi_2Sr_2CaCu_2O_{8+x}$. We further show our direct sensitivity to the temperature of the tunneling electrons at low voltages. Our MHz circuitry opens up the possibility to study charge and correlation effects at the atomic scale in all materials accessible to STM. © *2018 Author(s).*

I. INTRODUCTION

A direct consequence of the discreteness of the electron charge is the presence of time-dependent fluctuations of the electronic current, called shot-noise. In the tunneling limit, the power spectral density of the shot-noise is given by $S_I = 2q|I|F$, where q is the charge of the tunneling entity, I is the average current, and F is the Fano factor that encodes correlation effects (see Ref. 1 for a review of the theory and application of shot-noise measurements in mesoscopic systems). Particularly suited for mesoscopic systems, shot-noise has been a powerful tool in the study of electron-electron correlations in, e.g., Kondo systems[2–5] and Coulomb blockade scenarios[6,7] and has been used to reveal fractional charges in the fractional quantum hall regime,[8,9] as well as doubling of the charge transferred for Andreev tunneling.[10,11] The spatial resolution of these experiments is typically determined by the width of the contact leads to the sample and therefore ranges from tens of nanometers to several microns. This makes it impossible to study single impurities in a host material, for instance single atom Kondo physics, or correlation effects of impurities in doped Mott insulators such as the high-Tc cuprates. Previous efforts have shown the feasibility to increase the spatial resolution of shot-noise detection by using a scanning tunneling microscope (STM),[12–15] allowing for the study of junctions formed with nanometer sized metallic particles.[12] This is because the shot-noise is a current noise and will consequentially have the same atomically resolved resolution as the tunneling current in an STM. Most of these approaches relied on relatively high tunneling currents,[13–15] which due to the high local electric fields result in unstable junctions with many (weakly van der Waals bound) correlated electron systems.

Here we demonstrate our ability to measure shot-noise at the atomic scale at low currents (<1 nA) and high junction resistances (>10 MΩ) simultaneously with DC tunneling spectroscopy. We achieve this by combining a home-built low temperature scanning tunneling microscope with an LC_{cable} resonant circuit and a cryogenic amplifier based on a high electron mobility transistor (HEMT).[16] First, we describe the circuit in detail and present shot-noise measurements on a gold surface, which serves as a calibration of the circuit. We then show the sensitivity of shot-noise to the electron temperature and our ability to measure differential conductance at MHz modulation frequencies. We illustrate the capabilities of our atomic scale shot-noise microscope by simultaneously measuring the atomically resolved differential conductance and shot-noise on the high temperature superconductor $Bi_2Sr_2CaCu_2O_{8+x}$.

II. THE CIRCUIT

At low frequencies (<100 kHz), the noise spectral density is dominated by 1/f noise and mechanical resonances. At frequencies >100 kHz where shot-noise can be determined accurately, voltage noise from commonly used (high input impedance) room temperature current amplifiers is converted into current noise by the cable capacitances. As this spurious current noise grows linearly with frequency, it rapidly overwhelms the shot-noise. To overcome the impedance mismatch at low temperature and loss through cable capacitances, we have equipped our home-built scanning tunneling microscope [Fig. 1(a)] with a cryogenic low-noise high electron mobility transistor[16] [Figs. 1(b) and 1(c)]. To convert the current noise to voltage noise at the input of the HEMT, we use an LC_{cable} resonant circuit with its resonance tuned in the low MHz regime. The HEMT with input capacitance $C_{input} = 3.5$ pF is biased in saturation with $V_{dd} = 600$ mV, which, due to a total series resistance of 375 Ω (not shown), gives a current through the HEMT of approximately 1 mA and a gain of 7 dB (see calibration below). A capacitance (C = 6.8 nF) separates the
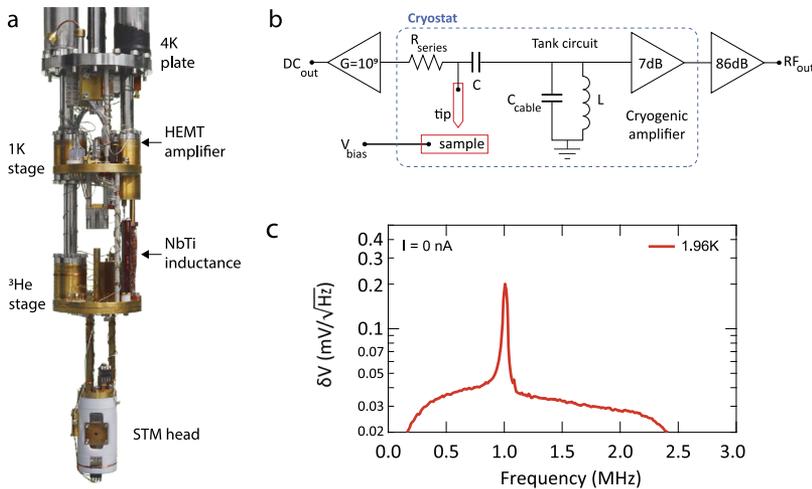
FIG. 1. MHz STM. (a) Home-built scanning tunneling microscope (design based on Ref. 17) outfitted with MHz circuitry. (b) In parallel to a conventional junction and its stray capacitance, R_J and C_J, respectively, a finite frequency circuit is added consisting of an LC_{cable} resonance and a HEMT amplifier. The inductance is a coil of superconducting NbTi wire with L = 155 μH, which gives a resonance at 1 MHz for a cable capacitance of $C_{cable} \sim 160$ pF. A capacitance, C = 6.8 nF, separates the DC and AC circuits, and a resistance, R_{series} = 400 kΩ, in series with the tunnel junction suppresses cross talk and ensures that the LC_{cable} resonance has a proper ground. A bandpass filter further removes the DC and high frequency components before readout with a spectrum analyser. (c) Thermal noise of the LC_{cable} resonance at T = 2 K.

current line from the LC_{cable} resonant circuit, enabling determination of the shot-noise simultaneously with conventional STM measurements. The current noise is converted to voltage noise at the HEMT input by the modulus of the impedance at resonance, $|Z_{res}|$. This impedance is set by the quality factor of the LC_{cable} resonance and the resistance, R_{series} = 400 kΩ, in the current line that suppresses cross talk between the two circuits and ensures that the LC_{cable} resonance has a proper ground.

As the conversion of current noise to voltage noise goes with the square of the impedance at resonance, whereas the Johnson-Nyquist (i.e., thermal) noise is linear in impedance, a higher impedance at resonance (i.e., higher quality factor) is beneficial. In order to have a relatively high impedance at resonance, yet still small compared to junction resistances of >10 MΩ typically used for studying correlated electron systems, we use a home-wound inductance of 155 μH made from Cu-clad NbTi wire which has an impedance at resonance of 170 kΩ (see below). The AC voltage noise output from the HEMT is further amplified at room temperature followed by a bandpass filter to remove 1/f and high frequency noise. The voltage noise at the spectrum analyser can then be approximated by

$$S_{tot} = (2q|I|F|Z_{res}|^2 + 4k_B T|Z_{res}| + \delta V_{amp}^2)G^2, \quad (1)$$

where G^2 is the total gain of the amplification chain, δV_{amp} is the combined input and output voltage noise of the various amplifiers, and T is the temperature of the LC_{cable} resonator, which we show to be identical to the temperature of the STM (T_{stm}) and of the tunnel junction (T_e).

III. CALIBRATION

To calibrate our circuit, we bring a Pt/Ir tip in tunneling contact with a gold sample. The shot-noise in this case is purely Poissonian, and the charge is equal to a single electron charge, i.e., F = 1 and q = e. In order to accurately determine the impedance at resonance, as well as the gain and the noise of the amplification chain, we measure the shot-noise of the junction for a range of temperatures between 1 K and 10 K. We use a sufficiently high junction resistance (>10 MΩ) to not be affected by thermal effects. We further assume that the quality factor of the resonant circuit (Q $\sim$ 25), which is at the same temperature as the sample and tip, is temperature independent below the superconducting transition temperature of NbTi, $T_c \sim$ 10 K. The temperature of the HEMT, which is mounted on a different stage, is kept below 5 K, where its input noise and gain can safely be assumed to be temperature independent.[16] Figure 2(a) shows the noise as a function of temperature in the
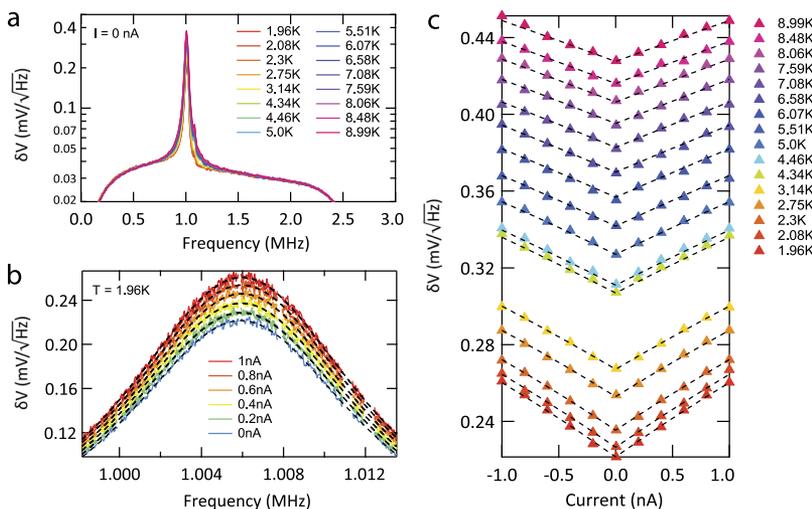

FIG. 2. Circuit calibration. (a) Thermal noise as a function of frequency for different temperatures. (b) Current dependence of the total noise at 2 K at a fixed junction resistance of 100 MΩ; dashed lines are Lorentzian fits to extract the peak amplitude. (c) Magnitude of the amplitude spectral density as a function of current for a range of temperatures; dashed lines are fits using Eq. (1) with $|Z_{res}|$ = 170 kΩ, G = 4.5 $\times$ 10^4 (G_{HEMT} = 2.25), and δV_{amp} = 2.42 nV/$\sqrt{Hz}$.

absence of a tunneling current, i.e., the thermal noise of the resonance plus the background noise of the amplification chain. Upon establishing a current, additional noise is observed, as can be seen for T ~ 2 K in Fig. 2(b), which is the shot-noise we are interested in. We fit the peak of the resonance with a Lorentzian [dashed lines in Fig. 2(b)] to extract its maximum value. Figure 2(c) shows the peak amplitudes of the total noise as a function of tunneling current for a range of temperatures—the value at I = 0 nA corresponds to the thermal noise plus the background from the amplification chain, as shown in Fig. 2(a). To extract all relevant circuit parameters, we finally fit the current and temperature dependence of Fig. 2(c) using Eq. (1), setting F = 1, giving: $|Z_{res}|$ = 170 kΩ, G = 4.5 × 10^4 (of which the gain of the HEMT, G_{HEMT}, is 2.25), and δV_{amp} = 2.42 nV/$\sqrt{Hz}$. Subsequent cooldowns have given similar results.

IV. ELECTRON TEMPERATURE

An additional benefit of our shot-noise scanning tunneling microscope is that through shot-noise, we are directly sensitive to the temperature of the tunneling electrons. At sufficiently low voltages, the shot-noise will become thermally limited, as can be appreciated from the full expression of the shot-noise, $S_I = 2q|I| \coth(eU/2k_B T_e)F$, where T_e is the electron temperature and U is the bias voltage. This temperature need not necessarily be identical to the bath temperature that is used in the fits to determine the circuit components (Fig. 2) as atomic scale Joule heating, or limited filtering, and/or poor thermal anchoring could lead to a higher junction temperature. In Fig. 3, we show shot-noise measured at R_J = 10 MΩ (E_{bias} = ±10 mV) for three different temperatures. Since at these relatively low voltages and high currents, the voltage drop over the series resistance in the current line (R_{series} = 400 kΩ) becomes non-negligible, we have taken into account that the voltage drop across the sample is reduced by a factor IR_{series}. As expected, once the voltage approaches the thermal energy of the electrons, $eU \sim 2 k_B T$, the noise levels off. The excellent match between the data and the fits (dashed lines) using $T_e = T_{stm}$ shows that our tip, sample, and the resonator are

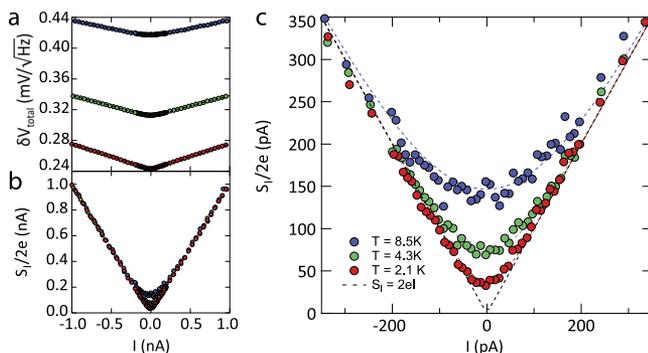properly thermalised to the bath and that at <1 nA current, Joule heating is negligible. Conversely, it proves that we can use shot-noise as an accurate thermometer of the tunnel junction.

V. ATOMIC RESOLUTION AND MHz MODULATION

We now proceed to demonstrate that we can atomically resolve spectroscopy and simultaneous shot-noise measurements and show the benefits of measuring differential conductance at finite frequency by turning our attention to the high temperature superconductor $Bi_2Sr_2CaCu_2O_{8+x}$ (Bi2212). Figure 4(a) displays the atomically resolved lattice of an optimally doped sample (T_c ~ 90 K) with its characteristic incommensurate super-modulation. Using a conventional low frequency (429.7 Hz) lock-in technique, we measure the differential conductance shown in Fig. 4(b). An additional voltage modulation with a frequency corresponding to the resonance frequency of our LC_{cable} circuit can be added to simultaneously measure the differential conductance at 1 MHz. As is apparent from Fig. 4(b), the elevated frequency of the lock-in detection enhances the signal-to-noise ratio significantly, reducing the required measurement time for spectroscopic measurements—in this case, the same signal-to-noise ratio can be achieved in more than a factor of three times less averaging.[18]

To measure the shot-noise simultaneously with the differential conductance as a function of spatial location, we reserve our MHz circuit for shot-noise detection, while applying a
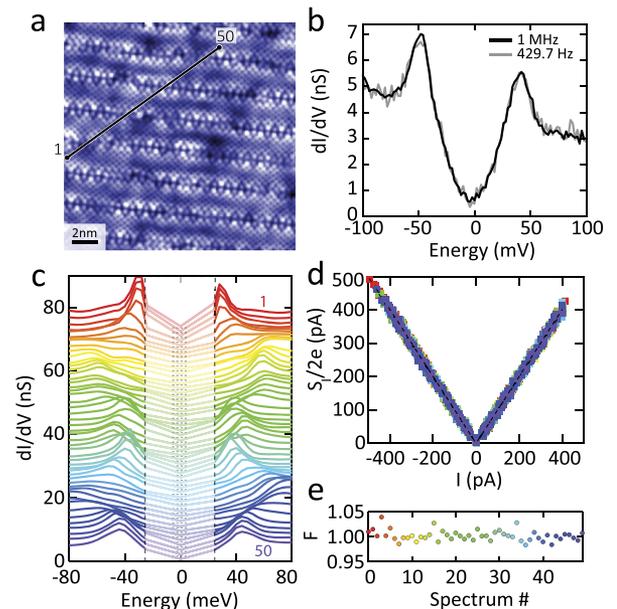
FIG. 4. (a) Atomic resolution image of $Bi_2Sr_2CaCu_2O_{8+x}$ taken with our MHz enabled STM. (b) Differential conductance using a voltage modulation of 1 mV at 429.7 Hz (DC circuit, demodulation time constant 4 ms) and 1 MHz (AC circuit, demodulation time constant 7.35 μs) with identical averaging times per point, taken simultaneously with each other. (c) Spatial variation of differential conductance spectra taken along the line indicated in (a), focussing on |E| > 30 mV. (d) Shot-noise measurements taken simultaneously with the spectra in (c). (e) Fano factor extracted from the slope of the shot-noise measurements in (d). Simultaneously taken measurements in [(c)–(e)] have the same colour.

FIG. 3. (a) Total voltage noise at three different temperatures for the same junction resistance of 10 MΩ. (b) Shot-noise after taking into account the thermal noise of the circuit (but not of the tunnel junction) and the noise of the amplification chain; see Eq. (1). (c) Enlargement of (b) corresponding to energies where the thermal noise of the junction becomes limiting (dots: measurement, coloured dashed lines: fits with $T_{fit} = T_{stm}$, and black dashed line: $S_I = 2e|I|$).

low frequency voltage modulation to determine the differential conductance. Figure 4(c) shows a series of spectra taken at various locations including regions of small ($\Delta_{peak-peak} \sim 30$ mV) to big ($\Delta_{peak-peak} \sim 70$ mV) gaps. All spectra are taken with a setup voltage and current of 80 mV and 400 pA, respectively. As the feedback loop is turned off and the voltage is swept from 80 mV to −80 mV, the current reduces to zero and changes sign, allowing us to simultaneously measure the current dependence of the shot-noise. The current in this case is predominantly from states outside the gap, i.e., $|E| > 30$ mV, and the corresponding shot-noise is presented in Fig. 4(d). Despite the large variation in the gap size of the various locations, the states outside the gap that we address here show little to no variation in their shot-noise—the slope of the noise, or the Fano factor, plotted in Fig. 4(e) is equal to one for all spectra with an error bar of a few percent. This means that outside the gap, the quasi-particles responsible for tunneling have a charge equal to a single electron charge, e, and tunneling events are uncorrelated within our experimental error, $F = 1$.

VI. DISCUSSION

We have shown our ability to resolve shot-noise at the atomic scale simultaneously with the conventional, DC operation of a scanning tunneling microscope at low currents and high junction resistances with an experimental uncertainty of a few percent in the slope of the noise. The MHz circuitry we have implemented in our home-built microscope to achieve this can in principle be installed onto any low temperature scanning tunneling microscope, making this technique widely applicable.

One of the crucial ingredients in our circuit is the use of an impedance matching cryogenic amplifier. Due to its very low input noise at low temperature ($\delta V_{input} = 0.22$ nV/$\sqrt{Hz}$ at 1 MHz), our cryoHEMT allows us to detect shot-noise with a high signal-to-noise ratio at low currents. For comparison, a low frequency circuit ($\sim$40 kHz) with room temperature amplification allowed us to detect the signs of shot-noise after averaging each data point for several minutes at currents up to 1 nA. The system described in this work achieves the same signal-to-noise ratio for sub-second averaging times. This can be further improved upon by suppressing the thermal noise at even lower temperature and/or by increasing the impedance at resonance.

In this work, we decided to keep our resonant frequency relatively low with a modest quality factor as this allows us to perform all measurements with a conventional STM controller down to junction resistances of a few MΩ without loss of signal. To reach higher resonant frequencies, two factors become important. The first is the quality factor of the LC_{cable} resonant circuit. For a fixed cable capacitance, a higher resonant frequency is achieved by implementing a smaller inductance. The quality factor, which goes as $\sqrt{L/C_{cable}}$, and thus the height of the resonance, therefore drops with increasing frequency, reducing the signal-to-noise ratio. The second is the capacitance of the tunnel junction itself, which is typically a few fF. The impedance of a junction with a capacitance of 3 fF will be comparable to the impedance of our resonance

($\sim$170 kΩ) at 300 MHz, providing an upper bound for the frequencies that can be reached with our circuit. To reach such frequencies requires a dramatic increase in the quality factor of the resonance, which may be achieved by implementing an inductance coil of pure superconducting wire, and complete elimination of all parasitic capacitances except the junction capacitance.

In order to address changes in the Fano factor with an even higher accuracy than a few percent reported here and/or for low junction resistances, i.e., when $R_J \gg Z_{res}$ does not hold, one important factor needs to be taken into account that was negligible in the measurements we have presented thus far. The voltage to ground at the input of the cryogenic amplifier is proportional to the impedance at resonance of the LC_{cable} circuit parallel to R_{series} *and* R_J. As the latter reduces, so does the absolute value of the detected noise as Z_{res} in Eq. (1) should be replaced by the transimpedance $Z_0 = Z_{res}R_J/(Z_{res} + R_J)$.[19] If the current-voltage characteristic is non-linear, as is the case, for example, for Bi2212, the dynamical resistance has to be substituted for R_J in this correction.

The atomic scale detection of shot-noise we present here opens up a new avenue to study the dynamics of tunneling and correlation effects around single impurities in all systems accessible by scanning tunneling microscopy.

Note: a similar approach for atomic scale noise detection is reported by Bastiaans et al.: "Amplifier for scanning tunneling microscopy at MHz frequencies."

[1]Ya. M. Blanter and M. Büttiker, Phys. Rep. **336**, 1 (2000).
[2]Y. Meir and A. Golub, Phys. Rev. Lett. **88**, 116802 (2002).
[3]T. Delattre, C. Feuillet-Palma, L. G. Herrmann, P. Morfin, J. M. Berroir, G. Fève, B. Plaçais, D. C. Glattli, M. S. Choi, C. Mora, and T. Kontos, Nat. Phys. **5**, 208 (2009).
[4]Y. Yamauchi, K. Sekiguchi, K. Chida, T. Arakawa, S. Nakamura, K. Kobayashi, T. Ono, T. Fujii, and R. Sakano, Phys. Rev. Lett. **106**, 176601 (2011).
[5]M. Ferrier, T. Arakawa, T. Hata, R. Fujiwara, R. Delagrange, R. Weil, R. Deblock, R. Sakano, A. Oguri, and K. Kobayashi, Nat. Phys. **12**, 230 (2016).
[6]A. N. Cleland, J. M. Schmidt, and J. Clarke, Phys. Rev. Lett. **64**, 1565 (1990).
[7]C. Altimiras, O. Parlavecchio, P. Joyez, D. Vion, D. Roche, D. Esteve, and F. Portier, Phys. Rev. Lett. **112**, 236803 (2014).
[8]R. de Picciotto, M. Reznikov, M. Heiblum, V. Umansky, G. Bunin, and D. Mahalu, Nature **389**, 162 (1997).
[9]A. Bid, N. Ofek, M. Heiblum, V. Umansky, and D. Mahalu, Phys. Rev. Lett. **103**, 236802 (2009).
[10]X. Jehl, M. Sanquer, R. Calemczuk, and D. Mailly, Nature **405**, 50 (2000).
[11]Y. Ronan, Y. Cohen, J. H. Kang, A. Haim, M. T. Rieder, M. Heiblum, D. Mahalu, and H. Shtrikman, Proc. Natl. Acad. Sci. U. S. A. **113**, 1743 (2016).
[12]H. Birk, M. J. M. de Jong, and C. Schönenberger, Phys. Rev. Lett. **75**, 1610 (1995).
[13]U. Kemiktarak, T. Ndukum, K. C. Schwab, and K. L. Ekinci, Nature **450**, 85 (2007).

[14]M. Herz, S. Bouvron, E. Cavar, M. Fonin, W. Belzig, and E. Scheer, Nanoscale **5**, 9978 (2013).

[15]A. Burtzlaff, A. Weismann, M. Brandbyge, and R. Berndt, Phys. Rev. Lett. **114**, 016602 (2015).

[16]Q. Dong, Y. X. Liang, D. Ferry, A. Cavanna, U. Gennser, L. Couraud, and Y. Jin, Appl. Phys. Lett. **105**, 013504 (2014).

[17]S. H. Pan, E. W. Hudson, and J. C. Davis, Rev. Sci. Instrum. **70**, 1459 (1999).

[18]The signal-to-noise ratio can be further improved upon by, e.g., reducing the parasitic stray capacitances.

[19]We can safely ignore the capacitance, C, since $Zc = 1/(2\pi f C) \sim 25\ \Omega$ is negligible.